Uncertainty and sensitivity analysis of the QUENCH-08 experiment using the FSTC tool

A. Stakhanova [a,*], F. Gabrielli [a], V.H. Sanchez-Espinoza [a], A. Hoefer [b], E. Pauli [c]

[a] Karlsruhe Institute of Technology, KIT, Hermann-von-Helmholtz-Platz 1, Eggenstein-Leopoldshafen, Germany
[b] Framatome GmbH, Seligenstädter Strasse 100, 63791 Karlstein am Main, Germany
[c] Framatome GmbH, Paul Gossen Strasse 100, 91052 Erlangen, Germany

ARTICLE INFO

Keywords:
ASTEC
Fast Source Term Calculation tool
QUENCH-08
U&S analysis

ABSTRACT

This paper presents results of a preliminary uncertainty and sensitivity (U&S) analysis of the QUENCH-08 experiment using the Fast Source Term Calculation (FSTC) tool, which currently is under development at KIT/INR as a part of WAME project. WAME is devoted to the development of a methodology and a tool for fast and accurate source term (ST) calculation in case of severe accident at nuclear power plant (NPP). The FSTC tool is divided into 2 parts: the U&S analysis and ST prediction (using the MOCABA approach), respectively. The description of the MOCABA approach, which is implemented in FSTC tool, will be presented – together with the results of ST evaluation – in a subsequent paper. In this paper, the FSTC tool is applied in conjunction with the Accident Source Term Evaluation Code (ASTEC) (version 2.2_b) severe accident (SA) code to the U&S analysis of the QUENCH-08 experiment to demonstrate the functionality of the tool and to check the methodology's suitability for the application to a nuclear power plant.

1. Introduction

The WAME project (supported by the Federal Ministry of Economics and Technology of Germany) is performed by Karlsruhe Institute of Technology (KIT) in cooperation with Framatome. The main goal of the project is to improve the decision making during severe accidents by delivering a methodology to accurately calculate radiological ST predictions in real time using pre-calculated data for different SA sequences and data from plant detectors measured during the accident. This methodology will be applied to a German KONVOI Pressurized Water Reactor (PWR) plant, first for a Medium Break Loss of Coolant Accident (MBLOCA) developed into SA. Taking into account the wide range of possible accident sequences, the above-mentioned pre-calculated data have to cover the uncertainty range of parameters characterizing the examined accident scenarios.

To achieve that, one of the important steps is to perform a U&S analysis, for which a list of uncertain input parameters potentially impacting the radiological ST prediction has to be identified, and their uncertainty ranges have to be estimated and parametrized in terms of probability density functions (PDFs). The input parameter uncertainties are then propagated to output parameter uncertainties by drawing Monte Carlo samples of the input parameters from their respective PDFs and performing accident calculations for each set of randomly sampled input parameters. By examining the simulation results, uncertainty bands for the output parameters of interest, as well as the magnitude of importance of the uncertain input parameters, can be estimated and identified. Many dedicated tools, like SUSA (Kloos and Hofer, 1999) and SUNSET (Chevalier-Jabet et al., 2014), or platforms, such as URANIE (Blanchard et al., 2019) and DAKOTA (Adams et al., 2014), exist for the quantification of uncertainties and the sensitivity to input parameters. However, it was decided to develop a new tool in order to have a work environment flexible enough to assess the ST database expected in the framework of the WAME project, to be employed later by the MOCABA procedure (Hoefer et al., 2015) for the ST updating based on measured plant data. This newly developed tool is named as FSTC. Its flexible structure enables a researcher to easily add, modify or remove different parts of its functionality and to investigate the performance of the Uncertainty Quantification (UQ) methodologies when applied to SA analyses. Such evaluations are also currently under investigation in the framework of the EU Management of Uncertainties in Severe Accidents (MUSA) project (MUSA, 2021; Herranz, 2020) and of the IAEA CRP I31033 'Advancing the State-of-Practice in Uncertainty and Sensitivity Methodologies for Severe Accident Analysis in Water Cooled Reactor' (Advancing the State-of-

* Corresponding author.
E-mail address: anastasia.stakhanova@kit.edu (A. Stakhanova).

Practice in Uncertainty and Sensitivity Methodologies for Severe Accident Analysis in Water-Cooled Reactors, 2021).

To test the methodology and its implementation in the FSTC tool, it is first applied to the evaluation of an integral bundle experiment – QUENCH-08 experiment (Stuckert et al., 2005)– in view of the application to SA analyses in a generic KONVOI plant by means of the ASTEC code (Chatelard et al., 2014). QUENCH-08 is a PWR bundle test which aims to assess the effect of degraded core cooling by steam and to examine oxidation and consequent hydrogen generation phenomena. The accident progression for the QUENCH-08 experiment is faster and less complex than for a nuclear power plant. The relatively short time of a single simulation (~1 h) makes it possible to run many different cases.

The structure of the paper is as follows. The FSTC code structure and its current functionality are described in section 2. The scheme of the QUENCH-08 experiment is briefly described in section 3. In section 4, the ASTEC models that were used in the simulations and the nodalization scheme of the QUENCH experiment facility are presented. In section 5, information about the input parameters for the ASTEC simulations, their meaning, uncertainty ranges and probability density functions are given. Section 6 is devoted to the discussion about choosing a sufficient number of samples. Results of the simulations with different numbers of samples are presented, as well as the results of consistency tests. The results of the uncertainty analysis for the QUENCH experiment are presented in section 7. Comparisons between results obtained with the FSTC tool and the URANIE platform are shortly presented in section 8. The paper is summarized with some conclusions and an outlook.

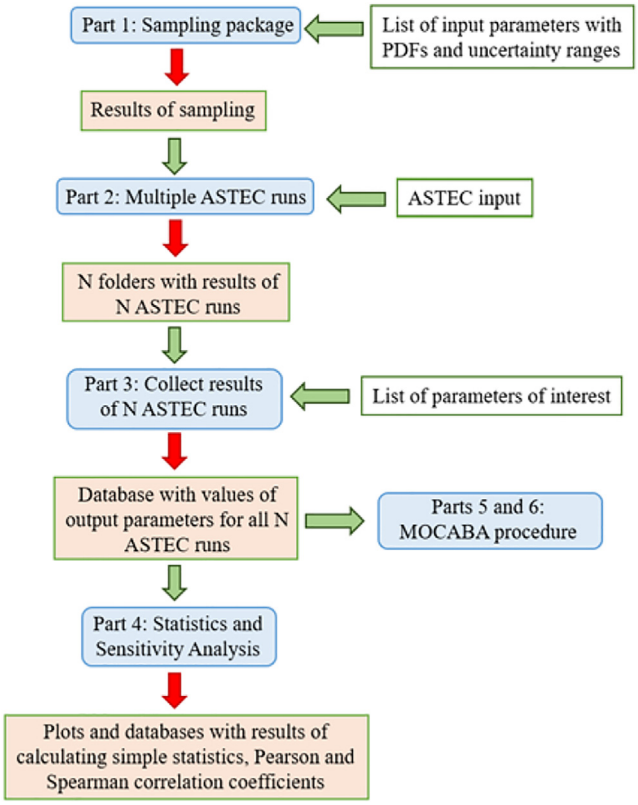

Fig. 1. Scheme of the FSTC tool.

2. The FSTC code structure

The FSTC code is written in the Python scripting language and currently consists of six parts:

1) **The Sampling** part uses the uncertainty information about the input parameters, their uncertainty ranges and related PDFs. The code generates random samples, writes the results of the sampling into a database and creates plots with sampling characteristics. Currently, only the Latin Hypercube Sampling (LHS) (McKay et al., 1979) method is used for the random sampling.
2) **The Running multiple simulations** part uses the ASTEC input deck and the results of part 1) as input data to create N copies of input for the ASTEC code, each copy with its own set of values of uncertain input parameters and after that runs N simulations in parallel. The code checks the number of cores and puts the runs in a simulation queue.
3) **The Collecting results of multiple runs** part collects values of all output parameters of interest from the ASTEC result files and checks that each ASTEC run from part 2) finished correctly. All results are stored in a database, which will be used later in parts 4), 5) and 6)
4) **The Statistics and Sensitivity Analysis part** uses data collected in the database from the previous part for calculating simple statistics, Pearson and Spearman correlation coefficients, and creating plots.

Parts 5) and 6) are devoted to the implementation of the MOCABA data assimilation procedure and will not be discussed in this paper. In Fig. 1, the computational scheme and the FSTC code structure are shown.

Please note, that words "samples" and "simulations" will be interchangeable along the whole text, but means the same – for example, "ASTEC simulations with 800 samples" and "800 ASTEC simulations" are equivalent. Following this example, it means that in input file for sampling part number 800 was specified, and 800 sets with uncertain input parameters values was created to be used in ASTEC runs. Each individual set from these 800 corresponds to its individual ASTEC run.

3. Quench-08 experiment

A Severe Accident is usually triggered by a lack of coolant supply to the core, i.e. Loss of Coolant Accident (LOCA), in conjunction with the loss most of the safety systems, i.e. Emergency Core Cooling Systems (ECCSs). In such conditions, the progression of the accident depends on the in-vessel thermal–hydraulic response, which may lead to the loss of the intact arrangement of the core. Following LOCA, the system is shut down and the decay power is being removed from the vessel by natural circulation. In absence of coolant supply, the core is exposed to vapor and the fuel rods temperature rapidly increases. Once the peak core temperature exceeds about 1500 K, the oxidation of the core components rapidly increases. Since the power produced by Zircaloy oxidation processes is comparable to the decay heat power, the oxidation phenomena are further triggered, leading to a large amount of hydrogen production. In order to terminate or mitigate the severe accident in Light Water Reactors (LWRs), water is injected to cool down the uncovered degraded core. Nevertheless, before the core cooling becomes efficient, Zircaloy oxidation processes may be enhanced. Further the rewetting (quenching) of the hot fuel rods is expected to cause the most severe consequences in terms of in-vessel hydrogen production. Note that the water injection in severe accident conditions is the most important Severe Accident Management (SAM) action in LWRs to terminate such abnormal events. Having this in mind, the QUENCH experimental program (including bundle and complementary separate-effects tests) was

therefore launched in 1997 at the KIT, formerly Karlsruhe Research Center (FZK) with the goal to analyze the in-vessel coolability phenomena and to evaluate the hydrogen production in pre-oxidized bundles.

The QUENCH-08 experiment was performed at KIT in 2003 to investigate the hydrogen generation in a pre-oxidized PWR rod bundle after quenching by water injection into the uncovered core. A detailed description of the experiment can be found in (Stuckert et al., 2005). The system pressure is 0.2 MPa. The test bundle consists of 21 fuel rod simulators (20 of them were heated electrically) and four corner rods – see cross-section of the bundle at Fig. 2. The cladding material, i.e. Zircalloy-4, and the dimension of each fuel rod are identical to that used in PWRs, a gas mixture of Ar and Kr filling the rod gap. The corner rods are composed of solid Zircaloy. The unheated central fuel rod is equipped with different devices, which allow performing quite accurate temperature measurements.

The experiment consisted of 6 phases (Fig. 3):

1. Heat-up to ~ 873 K up to 134 s from the beginning of the test;
2. Heat-up to ~ 1700 K with a rate of ~ 0.3–0.6 K/s up to 2277 s;
3. Pre-oxidation phase: constant temperature when superheated steam flowed through the test bundle up to 3240 s;
4. Transient phase: the temperature was increased up to 2200 K up to 3814 s;
5. Cooling down with saturated steam injected from the bottom of the test section starting from 3775.5 s up to the end of the test (4647 s);
6. Electric reduction from 3830 s up to 3.9 kW.

During the experiment, the temperatures of the simulator rods, shroud, etc. were measured with thermocouples at different elevations. The hydrogen mass was measured with a mass-spectrometer and a special hydrogen detection system at the bundle outlet. Also post-test examinations were made to investigate the oxidation and degradation processes in more detail.

4. Astec code model of quench-08 experiment

All simulations in this work were performed using the integral SA code ASTEC (version 2.2b), developed by the Institute de Radioprotection et de Sûreté Nucléaire (IRSN), which is continuously improved to analyse the complete SA scenario from the initiating event until radioactive release from the containment in Generation II and Generation III water-cooled reactors.

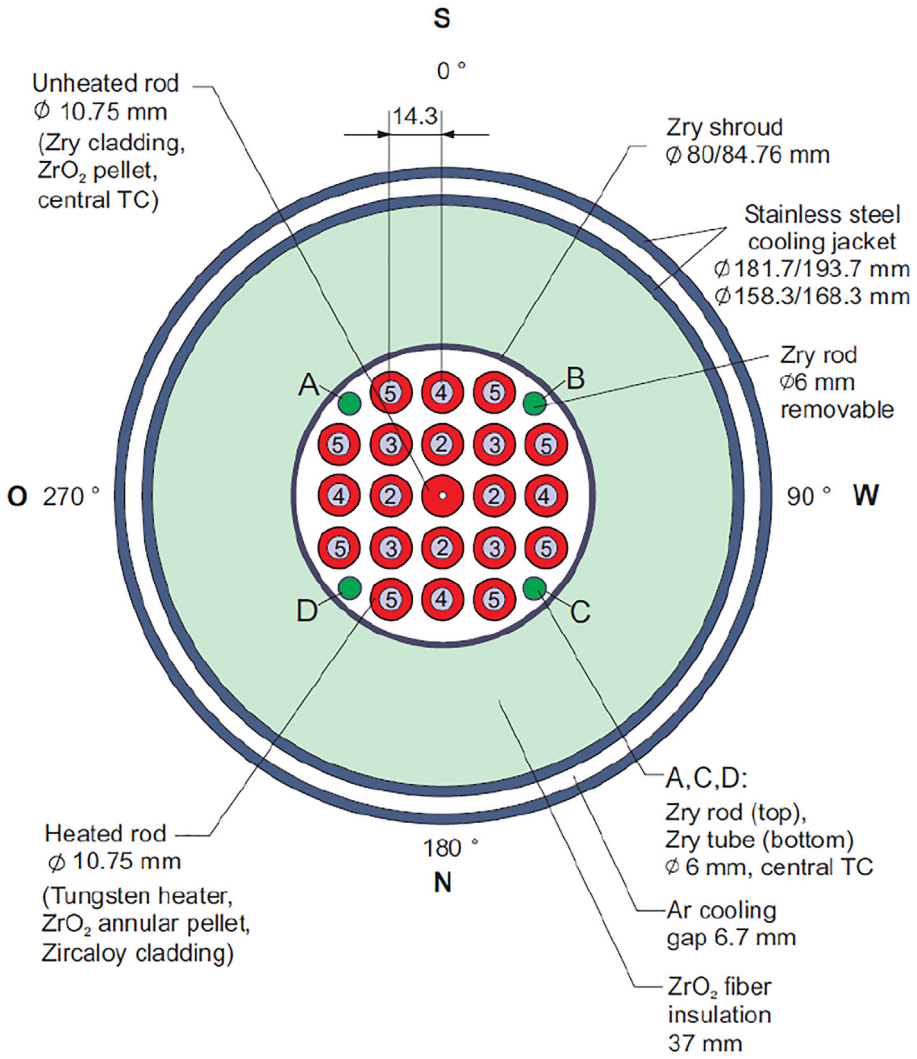

Fig. 2. QUENCH-08; Fuel rod simulator bundle (cross section, top view) and rod type designation. From (Stuckert et al., 2005).

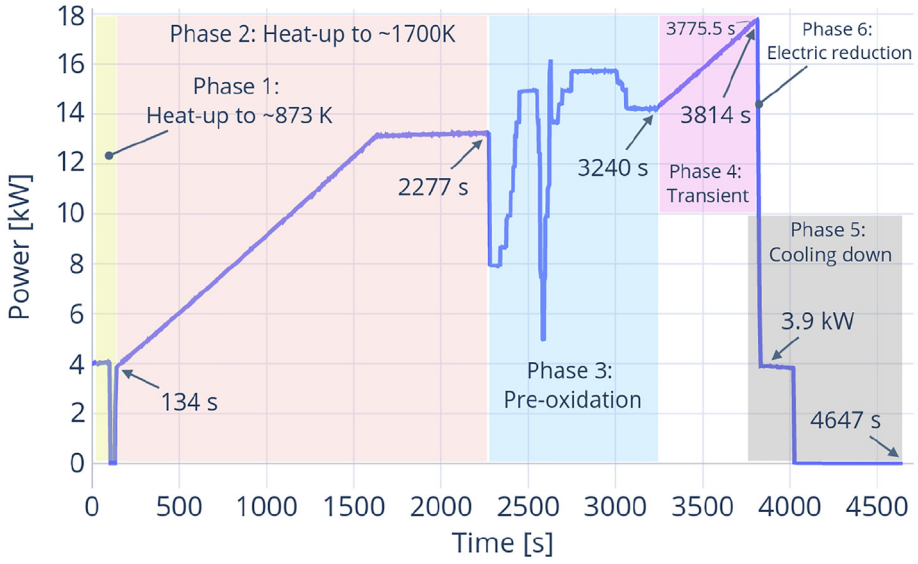

Fig. 3. Test conduct of QUENCH-08 experiment (see also Fig.19 in (Stuckert et al., 2005).

The ASTEC model of the QUENCH-08 experiment bundle consists of 21 fuel rods simulators and four corner rods arranged in two fluid channels: the central unheated rod plus the eight surrounding rods are connected to "Channel 1", and the other 12 heated rods plus the 4 corner rods are connected to "Channel 2" – see on the left part of Fig. 4. Further, the following structures have been also modelled: the five grid spacers, the shroud, the fiber insulation along the active zone (heated by means of W heaters), the Ar gap along the unheated length, and the inner tube of the annular cooling jacket. The model considers azimuthal symmetry at all times. The axial nodalization of the ASTEC model is shown in the right side of Fig. 4. The bundle is modelled by employing axial meshes of 55 mm height. Note that in Fig. 4, the *O2Zr* label refers to the ZrO_2 and *ZOFR* refers to the specific ZrO_2 alloy composing the fiber insulation.

As described in (Gómez-García-Toraño et al., 2017), the following assumptions have been made in the modelling:

- The tungsten heater is in contact with the fuel pellets, namely the radiation heat transfer from heater with unknown surface properties, e.g. roughness, is not considered;
- The four corner rods remain in their positions during the transient simulations, because the ASTEC code does not allow removing physical elements from the core during the calculation, while the corner rod B is extracted during the test;
- The electrical resistance between the electrode of each heated rod and the external cables is assumed to equal to 7 mΩ/rod (Stuckert et al., 2005);
- Conductive heat transfer is defined between the shroud and the cooling jacket through the argon gap, since direct radiative transfer between these two regions cannot be directly evaluated by ASTEC. The gap is therefore assumed to be a solid Ar cell, whose thermal resistance is continuously updated during the simulation to take into account the radiative and convective exchange between shroud and cooling jacket. Such approach is valid as long as the temperature gradient between such regions remains rather small, since the average temperature of the argon cell is properly calculated.

Time-dependent boundary conditions have been employed in the ASTEC model according to the experimental measurements (Stuckert et al., 2005): electrical power generated in the inner and outer rings; pressure and temperature of the inlet fluid; mass

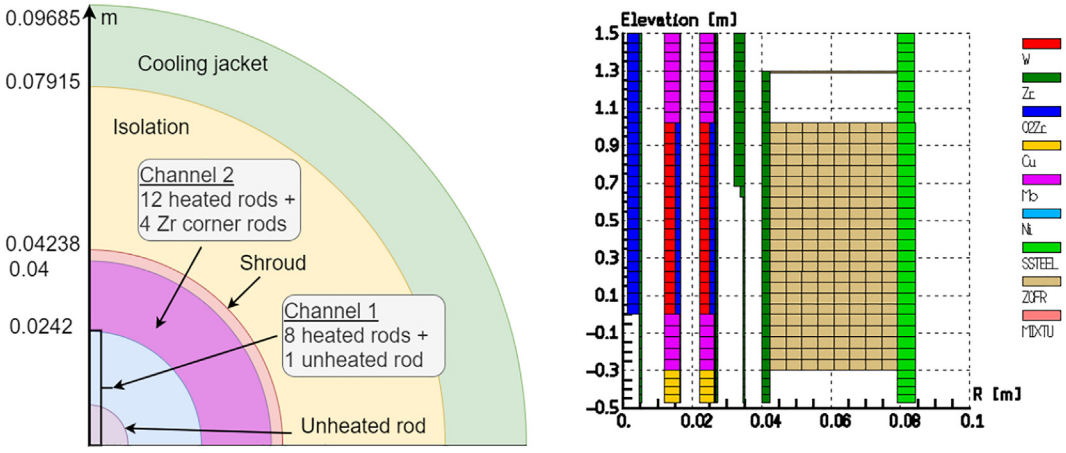

Fig. 4. Radial and axial nodalizations of QUENCH-08 in ASTEC.

of inlet fluid (see figure test conduct); axial temperature profile of the external surface of the cooling jacket according to the thermocouple experimental data. The reflooding occurs in the model at the same time as in the experiment, i.e. 3776 s.

The ASTEC model has been validated against the QUENCH-08 experiments. The results concerning the hydrogen production are shown in Fig. 5. The results show that ASTEC is able to rather well reproduce the mass of hydrogen generated during the experiment.

5. Input parameters uncertainties

For the uncertainty analysis, the selection of the uncertain input parameters, the specification of their uncertainty ranges and the parameterization of the uncertainties in terms of PDFs were based on previous U&S analysis of the CORA-W2 (Kobzar, 1997) and QUENCH-08 experiments performed at KIT (Gabrielli and Sanchez, 2018), the QUENCH-08 experiment report (Stuckert et al., 2005), and the ASTEC code documentationBelon, SAG/2016-00421, 2017.; Coindreau, PSNRES/SAG/2016-00422 (Belon, et al., 2017; Coindreau, 2017). These parameters are listed in Table 1. Note that, for a better clarity of the input deck while debugging, the uncertainty of some ASTEC parameters has been assessed by applying PDFs with mean value equal to the unity to the corresponding default values employed in the code.

Engineering judgments have been employed to assess the uniform PDFs and the min/max values for representing the uncertainty of the ASTEC parameters related to the corium behavior and the steam oxidation (Kobzar, 1997; Gabrielli and Sanchez, 2018). The uncertainty on the integrity criteria of the oxide layer of the cladding has been set based on the analysis of the results of the behavior of the early phase degradation of the fuel rods in the Phébus experiments (de Luze et al., 2013). According to the recommendationsBelon, SAG/2016-00421, 2017.; Coindreau, PSNRES/SAG/2016-00422 (Belon, et al., 2017; Coindreau, 2017), fuel rod failure occurs when the ZrO_2 temperature exceeds 2300 K or the oxide layer thickness is above 250 μm. In particular, a uniform PDF is employed to describe the uncertainty on the temperature threshold for the failure of the ZrO_2 layer, the PDF ranging from 2248 K (the ZrO_2 solidus temperature) to 2500 K. Further, we also consider that the failure may occur with the same probability in the range of the oxide layer thickness 200–400 μm, in order to take into account possible local effects in the QUENCH bundle.

The PDFs and the related parameters for the geometry parameters have been set on the base of engineering judgment as in (Kobzar, 1997). Normal PDFs have been employed for describing the uncertainties of the boundary conditions of the experiment, the standard deviation σ being set equal to the experimental error, which ranges from 2% to 5%.

The parameters governing the ASTEC physical models for the radiative heat transfers are assumed to be affected by large uncertainties in order to evaluate their effect on the most important Figure-of-Merit (FoM) of the QUENCH tests, namely the hydrogen production. Uniform PDFs are set for the related parameters (*frani* and *fsani* in Table 1), the uncertainty covering the full range of the allowable values in ASTEC. Concerning the convective heat transfer parameters, normal PDFs with σ = 5% around the default value in the code are employed for the *fhd* and *fzd* parameters. It is therefore assumed that such phenomena have the same uncertain behavior as the experimental boundary conditions.

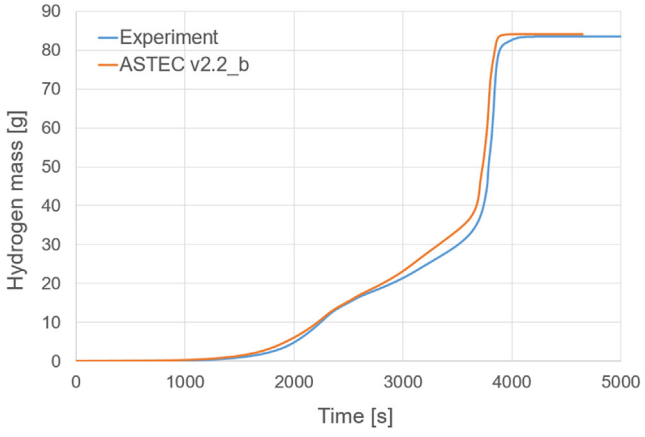

Fig. 5. Hydrogen mass – ASTEC simulation and experimental results.

6. Choice of sufficient number of samples

The assessment of a 'reliable' U&S methodology to be applied to SA codes is an open issue, which is, among others, one of the research activities currently going on in the framework of the EU MUSA project (MUSA, 2021; Herranz, 2020). Having this in mind, a preliminary study is performed here to evaluate the effect of the number of samples in the QUENCH-08 U&S analysis, in view of the application of the FSTC/ASTEC platform to SA analysis in a generic KONVOI plant.

In this framework, we focus our attention on the hydrogen production during the QUENCH-08 test and to the Pearson correlation coefficients for each input parameter during the transient. Such information is relevant to identify the uncertainties of the physical models employed in the SA codes (ASTEC in our case) governing the different stages of a SA scenario and then to produce, with enough level of confidence, the database for the MOCABA tool, which is the goal of the WAME project.

In order to estimate the joint PDF of the output parameters, a sufficient number of samples has to be chosen for the random sampling. It should be mentioned that the choice of the sufficient number of samples also depends on the available computational resources taking into account that computational time should stay reasonable.

In our case one simulation of the QUENCH-08 experiment takes ∼ 1 h, and it was possible to run up to 32 simulations in parallel. Based on that, the upper limit of the number of simulations was set to ∼ 1000.

A common criterion for choosing the number of samples is based on the minimum required value for calculating a tolerance region with a given coverage and a given confidence level. For this purpose, the well-known distribution-free method by Wilks (Wilks, 1941) is commonly employed. Wilks' method has also been generalized to the multivariate case (Wald, 1943; Tukey, 1947). One should also mention, that other metrics exist, which can help to define a sufficient number of samples to solve a problem, i.e. the L2-star discrepancy (Water Programming: A Collaborative Research Blog, 2021; SampleVis; Sheikholeslami and Razavi, 2017). The values of the metrics decrease with increasing number of samples.

The choice of the metrics therefore (and obviously) depends on the quantities we want to estimate from the sample data and on the precision we want to achieve. In our analysis, we compare the effect of employing different numbers of samples on the hydrogen production during the test and on the Pearson correlation coefficients. According to the Wilks' method, we employ 100 samples to achieve a coverage of 95% and a confidence level of 95% of such quantities (the minimum required number of samples is 93 for calculating two-sided tolerance intervals). In addition we considered 50, 200, 400, 600, and 800 samples.

Table 1
Input parameter probability density functions.

Parameter	PDF	PDF parameters	Description	Source
Parameters of the corium relocation model				
CRES	Uniform	[0.8 – 1.20]	Coefficient to modify the residual saturation	(Kobzar, 1997; Coindreau, 2017)
KEXP	Uniform	[2. – 4.]	Exponent for the saturation in the relative permeability	(Kobzar, 1997; Coindreau, 2017)
KSMX	Uniform	[0.9 – 1.10]	Maximum value of the ratio permeability/viscosity (sampled value is multiplied by 0.1 in the ASTEC input file)	(Kobzar, 1997; Coindreau, 2017)
Parameters of the model of melt oxidation by steam				
GRDR	Uniform	[0.9 – 1.10]	Corrective factor for the gradient in the crust interfacing with the liquid (sampled value is multiplied by 6.0 in ASTEC input file)	(Kobzar, 1997; Coindreau, 2017)
GREX	Uniform	[0.9 – 1.10]	Corrective factor for the gradient in the crust interfacing with the steam	(Kobzar, 1997; Coindreau, 2017)
HSLX	Uniform	[0.9 – 1.10]	Maximum value for the mass transfer coefficient between solid and liquid (sampled value is multiplied by 0.1 in ASTEC input file)	(Kobzar, 1997; Coindreau, 2017)
MULT	Uniform	[0.9 – 1.10]	Multiplying factor applied on the exchange area	(Kobzar, 1997; Coindreau, 2017)
OXLQ	Uniform	[0.9 – 1.10]	Factor for increasing/decreasing the external oxygen flux to the pure liquid when all the crust has disappeared	(Kobzar, 1997; Coindreau, 2017)
RDZR	Uniform	[0.9 – 1.10]	Relative diffusivity of Zr in the melt. (sampled value is multiplied by 0.01 in ASTEC input file)	(Kobzar, 1997; Coindreau, 2017)
Parameters of integrity criteria				
ZrO2T	Uniform	[2248. – 2500.] K	Failure temperature of ZrO_2 layer [K]	(Stuckert et al., 2005); (Gabrielli and Sanchez, 2018)
ZrO2Thi	Uniform	[200-400] 10^{-6} m	Thickness of ZrO_2 layer [m]	(Stuckert et al., 2005); (Gabrielli and Sanchez, 2018)
Geometry parameters				
d_int	Uniform	[0.99 – 1.01]	Parameter used to calculate internal diameters in the ASTEC nodalization of the QUENCH-08 experiment test bundle	(Stuckert et al., 2005); (Gabrielli and Sanchez, 2018)
s_thic	Uniform	[0.99 – 1.30]	Parameter related to the shroud thickness used to calculate geometric parameters in the ASTEC nodalization of the QUENCH-08 experiment test bundle	(Stuckert et al., 2005); (Gabrielli and Sanchez, 2018)
j_thic	Uniform	[0.99 – 1.01]	Parameter related to the cooling jacket thickness used to calculate geometrical parameters in the ASTEC nodalization of the QUENCH-08 experiment test bundle	(Stuckert et al., 2005); (Gabrielli and Sanchez, 2018)
Initial and boundary condition parameters				
stFlow	Normal	$\mu = 1., \sigma = 0.05$	Coefficient used to calculate the steam flow value at different time points	(Stuckert et al., 2005); (Gabrielli and Sanchez, 2018)
arFlow	Normal	$\mu = 1., \sigma = 0.05$	Coefficient used to calculate the argon flow value at different time points	(Stuckert et al., 2005); (Gabrielli and Sanchez, 2018)
cTime	Uniform	[0. – 10.] s	Possible delay of steam injection [s]	(Stuckert et al., 2005); (Gabrielli and Sanchez, 2018)
fpres	Normal	$\mu = 1., \sigma = 0.02$	Output pressure of the test bundle [Pa] (sampled value is multiplied by $2.0 \cdot 10^5$ in input ASTEC file)	(Stuckert et al., 2005); (Gabrielli and Sanchez, 2018)
fpp	Uniform	[0.99 – 1.01]	Argon pressure in the gap	(Stuckert et al., 2005); (Gabrielli and Sanchez, 2018)
Radiation heat exchange parameters				
frani	Uniform	[0. – 1.]	Rod reflection anisotropic factor	(Gabrielli and Sanchez, 2018; Coindreau, 2017)
fsani	Uniform	[0. – 1.]	Shroud reflection anisotropic factor	(Gabrielli and Sanchez, 2018; Coindreau, 2017)
Convective heat transfer model parameters				
fhd	Normal	$\mu = 100., \sigma = 0.05$	Average additional heat transfer coefficient due to droplet projection	(Gabrielli and Sanchez, 2018; Coindreau, 2017)
fzd	Normal	$\mu = 0.8, \sigma = 0.05$	Height above the quench front concerned by droplet projection	(Gabrielli and Sanchez, 2018; Coindreau, 2017)
falpha	Uniform	[0.99 – 0.999]	Threshold void fraction to allow exchange with liquid droplets	(Gabrielli and Sanchez, 2018; Coindreau, 2017)

The LHS method was chosen for random sampling of the input parameters by employing the open-source pyDOE Python library (pyDOE, 2021). For all simulations, the sampling was run with the criterion 'center', i.e. the points are centered within the sampling intervals.

For the hydrogen mass distribution we look at the mean, the 5th and the 95th percentiles. In case of the Pearson correlation coefficients between hydrogen mass and input parameters we look at its variation in time.

The results for the 95th percentile of the hydrogen mass for different numbers of samples is shown in Fig. 6. As expected, the effect of employing more than 100 samples is rather small. The deviation from the total amount of hydrogen predicted for the 100 samples case is ~ 5 g.

On the contrary, the results for the time-dependent Pearson correlation coefficients are affected by the number of samples set in the problem. According to our results, the mass of hydrogen is mainly affected by the steam and argon flow. The Pearson correlations for the corresponding parameters (*arFlow* and *stFlow*) are shown in Fig. 7.

In general, the results show that both parameters are anti-correlated with respect to the hydrogen generation (negative Pearson coefficients), namely an increase of the flow rates leads to a decrease of the hydrogen production. Such a behavior is expected,

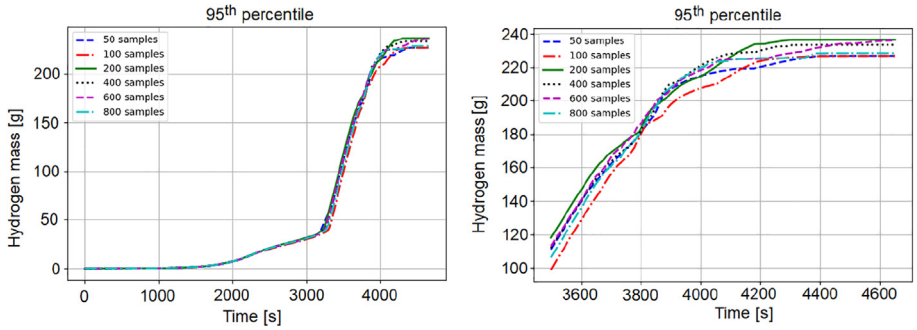

Fig. 6. Results of ASTEC simulations with different number of samples. 95th percentile values of the hydrogen mass produced during experiment.

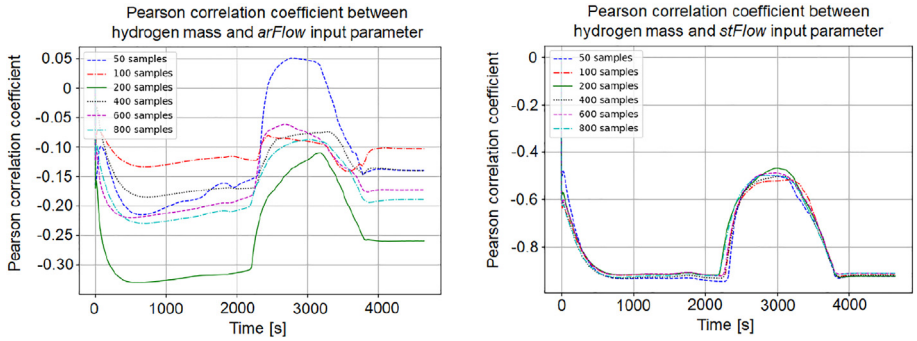

Fig. 7. Time-dependent Pearson correlation coefficients between hydrogen mass produced during experiment and the *arFlow* and *stFlow* parameters (cases with different numbers of samples).

since cladding oxidation phenomena are enhanced in case of loss of cooling. The results in Fig. 7 show that the *stFlow* Pearson coefficients are higher (in absolute value) than the corresponding values for the *arFlow* parameter. Namely, the hydrogen production is mainly influenced by the uncertainty of the steam mass flow rate than that of the argon flow rate. Such discrepancy is due to the different thermal properties of both coolants. In particular, the specific heat capacity of steam in the experiment condition is about four times higher than that of argon.

Furthermore, the results in Fig. 7 show that the employment of a different number of samples has a big impact on the Pearson correlations of the *arFlow* parameter. In particular, the lowest values of the Pearson correlation of the *arFlow* parameter during the transient range between −0.1 to −0.3 depending on the number of samples employed. On the contrary, no remarkable effect is observed for the *stFlow* parameter. Such different behavior results from the above mentioned different properties of argon and steam. The higher cooling efficiency of the steam with respect to argon makes the Pearson coefficients of the *stFlow* parameter rather independent on the sampling. On the contrary, the lower cooling performance of argon makes the results mainly dependent on the capability of covering the full space of occurrences during the random sampling. With this respect, the results of the consistency tests described below reveal that the time-dependent behavior of the Pearson correlation coefficients of the *arFlow* parameter looks independent on the sampling when more than 400 samples are employed.

The shape of the Pearson coefficients in Fig. 7 has been also investigated. In the next, the *stFlow* parameter will be considered. The results show that the Pearson coefficient decreases up to −0.9 and remains constant up to the end of the pre-heating phase (∼2280 s). Then, it increases up to about −0.5 during the pre-oxidation phase and the transient phase, and finally comes back to −0.9 after the steam flooding (∼3800 s). In order to investigate such behaviour, the hydrogen production computed for 600 samples is shown in Fig. 8. The results show that part of the simulations predicts a rapid increase of the hydrogen mass at the beginning of the pre-oxidation phase due to low values of the steam mass flow rate, which has been sampled in these calculations.

The scatter plots of the hydrogen production as function of *stFlow* samples at different instants during the transient are shown in Fig. 9. The results in the pre-oxidation phase (at 1500 s) show a good linear relationship between the hydrogen mass and the *stFlow* parameter. As a result a rather high values of the Pearson correlation is obtained (−0.9). During the pre-oxidation phase, part of the samples show a much higher hydrogen productions than the others corresponding to low values of the *stFlow* as shown by the

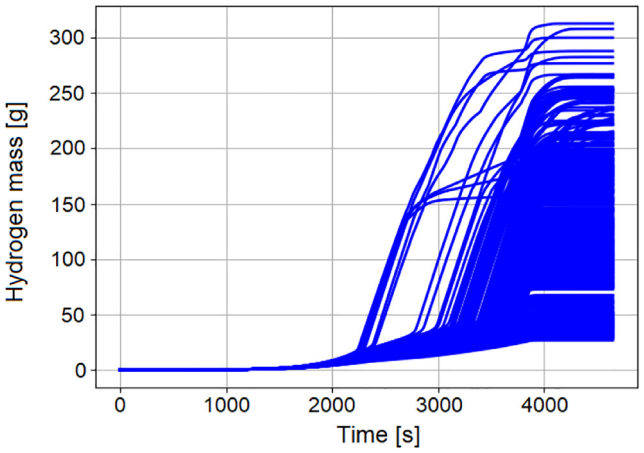

Fig. 8. Hydrogen production from 600 samples.

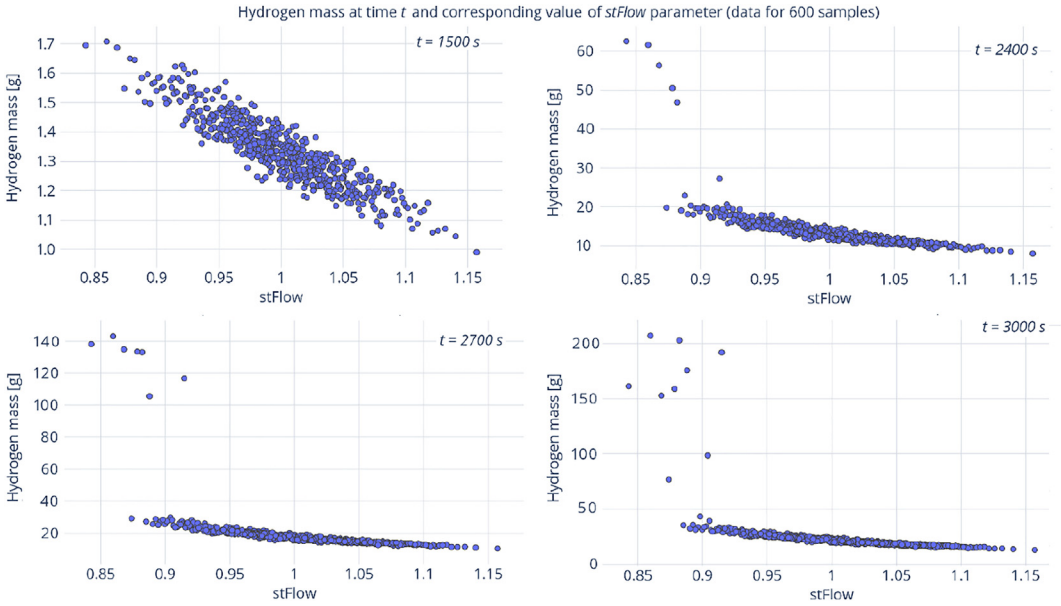

Fig. 9. Hydrogen production as function of the sampling of the *stFlow* parameter at different instants (600 samples).

plots at 2400 s, 2700 s, and 3000 s in Fig. 9. In these cases, the hydrogen mass and the *stFlow* parameter show a weaker linear correlation than in the previous phase. Therefore, if the whole population of samples is considered, the Pearson coefficients of *stFlow* will decrease (in absolute value) at 2400 s, 2700 s, and 3000 s up to about −0.7, −0.55, and −0.5, respectively, as shown in Fig. 7.

In order to analyse the results in the pre-oxidation phase, the Spearman correlations coefficients between the hydrogen production during the transient and the *arFlow* and the *stFlow* parameters have been evaluated. The results are shown in Fig. 10. By comparing with Fig. 7, it may be observed that the application of the Pearson and Spearman correlations provides rather similar time-dependent results in the pre-heating and post-flooding phases. On the contrary, the results from the beginning of the pre-oxidation phase to the instant of flooding (∼2280 s - ∼3800 s) show some discrepancies. In particular, the application of the Spearman correlation to the results in Fig. 9 reveal a rather strong monotonic relationship between the hydrogen mass produced during the experiment and the *stFlow* parameter, the values lower than −0.9.

The results therefore show that the employment of the number of samples evaluated based on the Wilks' method seems enough to estimate with sufficient precision the value of the FoM. On the contrary, attention has to be paid to this parameter in a U&S methodology when the effect of each single uncertain parameter on the FoM has to be evaluated. Furthermore, the analysis of the database by employing different correlations looks a rather powerful approach to identify possible relationships between input parameters and FoMs. Note that these tasks are of relevance in the application to SA codes in view of the reduction of the uncertainties associated to the physical models employed to model SA scenarios.

As a further analysis, a consistency test has been performed by re-running five times the FSTC/ASTEC coupling procedure with the same number of samples (50, 200, and 400). Note that the LHS method is employed for all simulations and that list of uncertain input parameters, as well as their PDFs and PDFs parameters always stayed the same.

Fig. 11 shows results of that test presenting the values for the 95th percentile and the Pearson correlation coefficient between hydrogen mass and the input parameters *arFlow* and *stFlow*. As expected, the results for the 95th percentile values for the hydrogen production are in good agreement for the different samplings. On the contrary, the Pearson correlation coefficients are quite sensitive to the re-sampling, in particular for the *arFlow* parameter. The results become more consistent with increasing number of samples. Concerning the *stFlow* parameter, the results show that 50 samples are not enough to have a consistent picture, while no significant deviations are observed when larger numbers of samples are employed.

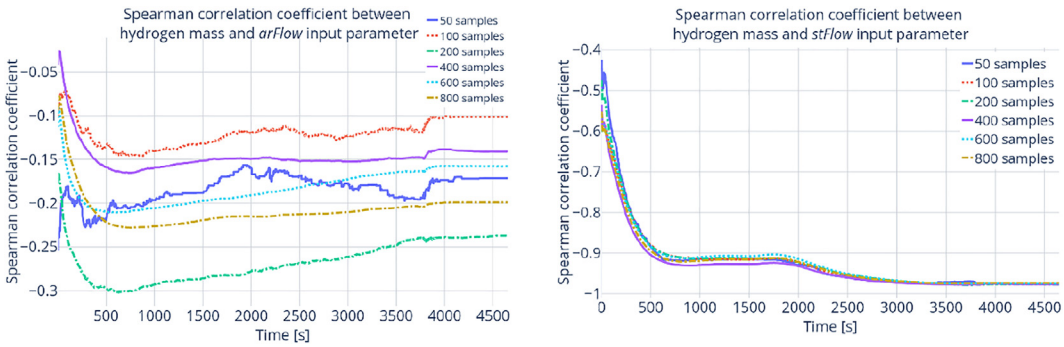

Fig. 10. Time dependent Spearman correlation coefficients between the production and the *arFlow* and *stFlow* parameters for different number of samples.

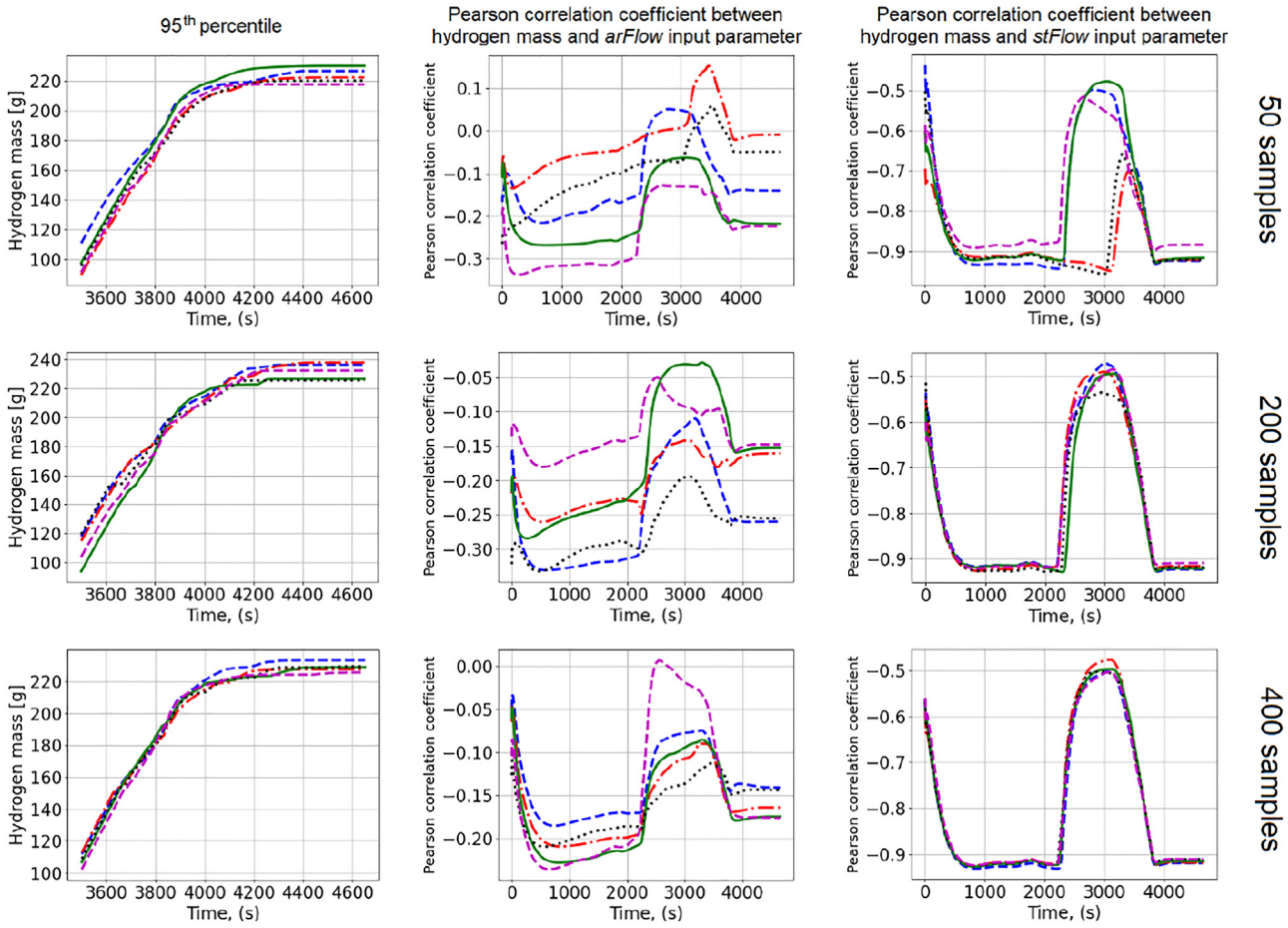

Fig. 11. Results of consistency test for 50, 200 and 400 samples (for each number of samples simulations were repeated 5 times).

Effects observed at the Fig. 11 are more likely to be happening due to random effects of sampling. Each time the user re-runs the sampling algorithm with exactly the same input, it is producing slightly different results because of shuffling procedure, which guarantees that the correlation between uncertain input parameters tends to zero. That leads to different combinations of sampled input parameters values.

7. Results of U&S analysis

The main results of the U&S analysis for the QUENCH-08 test are provided by running 800 ASTEC simulations using the FSCT tool. The 5th, 50th and 95th percentile, the arithmetical mean values and the experimental results for hydrogen mass are presented on Fig. 12. As one can see from the figure, the mean and median values from 800 simulations are quite close to the experimental results. Both the 5th and 95th percentile values are far from experiment and representing the effect of uncertainty of input parameters on ASTEC simulation results.

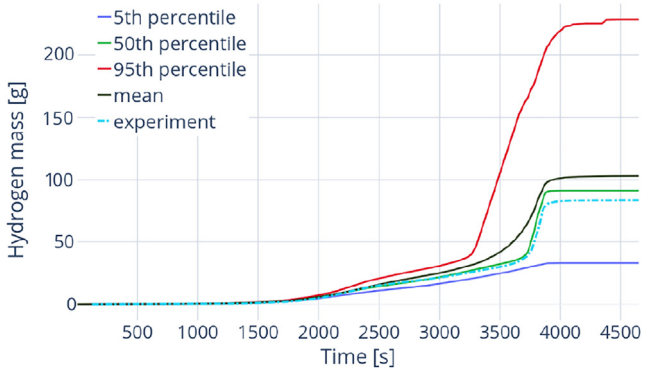

Fig. 12. Simple statistics values of ASTEC simulation results (800 samples) and experimental results for hydrogen mass.

In Fig. 13, the Pearson and Spearman correlation coefficient values between total mass of hydrogen produced in the test and the input parameters at the last time step are presented. The results show that the uncertainties of the *stFlow* and the *arFlow* parameters mainly affect the hydrogen production during the experiment. It seems reasonable in a next steps of the work to exclude most of the unimportant parameters from Table 1 having low correlations with the hydrogen mass and re-run the simulations.

The results in Fig. 13 show that the Pearson coefficients of the *stFlow* and *arFlow* parameters at the last time step are −0.9 and −0.2, respectively. Furthermore, the Spearman coefficients of *stFlow* and *arFlow* at the last time step are −0.98 and −0.2, respectively. Namely, an increase of the argon and steam mass flow rates leads to a reduction of the hydrogen production in the bundle. As also described above, the results in Fig. 13 show that such behaviour is mainly due to the cooling by steam, because of the high correlation coefficients. At the same time, because of the lower cooling capabilities of argon with respect to steam, the correlation coefficients of the *arFlow* parameter are about one fourth of the corresponding values of the *stFlow*.

A local and short-time occurrence of steam starvation phenomena over some period during the transient phase of the QUENCH-

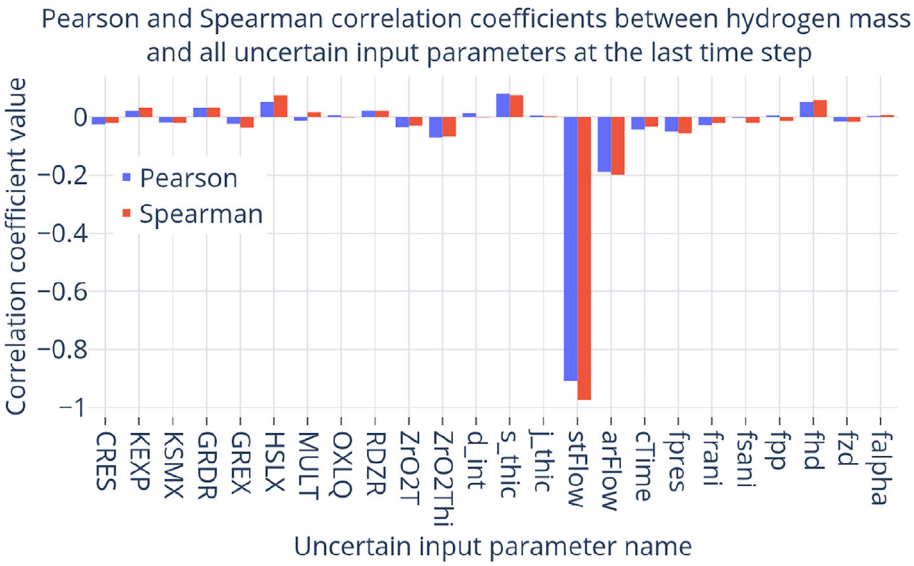

Fig. 13. Pearson and Spearman correlation coefficients between hydrogen mass and input parameters at the last time step.

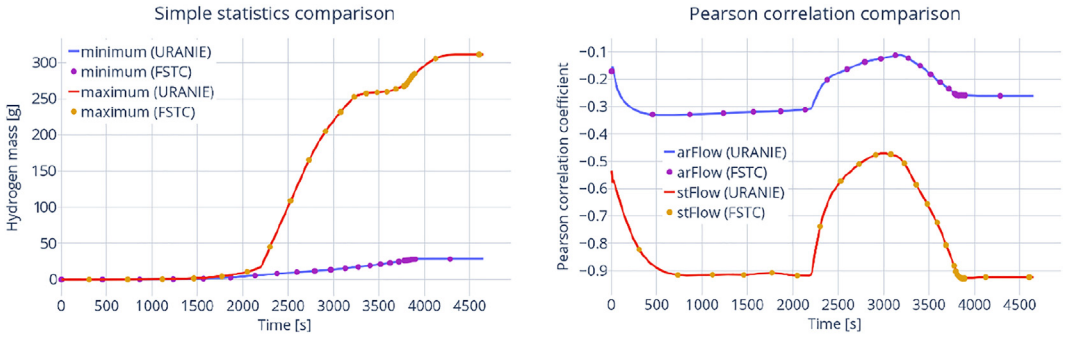

Fig. 14. Comparison between FSTC and URANIE. Minimum and maximum values of the hydrogen mass – on the left. Pearson correlation coefficients between hydrogen mass and *arFlow* and *stFlow* input parameters – on the right.

08 test has been considered by the QUENCH experimental team as the most credible speculation to explain the temperature escalation observed after the steam flooding in the upper part of the bundle (Stuckert et al., 2005). As also shown in (Gómez-García-Toraño et al., 2017; Gómez-García-Toraño, 2017; , xxxx), the ASTEC code predicts the experimental temperature and oxide layer behaviour at different elevations in the bundle. In general, when starvation takes place, the larger is the steam flow rate the higher is the hydrogen produced, since more oxidant material is available for the zircaloy cladding. Therefore, if such phenomenon is predicted by the ASTEC code, it may be expected a positive correlation between the coolant flow rates and the hydrogen mass produced, instead of the negative values of the correlations as shown above. Nevertheless, it should be noted that the FoM analysed here is the total amount of hydrogen produced during the transient. In order to analyse local effects, other FoMs should be considered, i.e. cladding temperature at elevations higher than 950 mm, mesh-wise hydrogen production.

8. Comparison with URANIE

The correctness of the FSTC tool has been verified by comparing results obtained with the FSTC tool to those obtained with URANIE (Blanchard et al., 2019). For this goal, the ASTEC/URANIE coupling at KIT (Gabrielli and Sanchez, 2018) has been employed. The test was performed creating the set of results of 200 ASTEC simulations of QUENCH-08 experiment, and providing that results as input data for both FSTC and URANIE tool to perform U&S analysis and calculate simple statistics. The FSTC and URANIE results for the minimum and maximum hydrogen mass and the Pearson correlations for *arFlow* and *stFlow* are shown in Fig. 14 on the left and the right side respectively.

One may observe that the results produces by FSTC and URANIE are identical, which proof that functionality implemented in the FSTC code is working correctly. FSTC therefore appears to be a suitable tool for the U&S analysis in the framework of the WAME project.

9. Conclusions and outlook

In this work, a preliminary U&S analysis of the QUENCH-08 experiment using the newly developed FSTC tool as part of the WAME project was presented and discussed. In order to perform such an analysis, the uncertain input parameters and their uncertainty ranges have been defined and parameterized in terms of PDFs, the FoM being the hydrogen mass produced during the QUENCH-08 transient.

The FSTC tool and the methodology have been tested with respect to different numbers of samples and re-sampling with fixed sample number. The results for the FoM show a high degree

of consistency. On the contrary, the sensitivity analysis reveals a significant dependence of the results on the number of samples employed. The FSTC tool has been verified against URANIE, the results showing a very good agreement with respect to the estimation of the FoM and the sensitivity coefficients. Having this in mind, this work is a solid basis for the next steps of the work activity in the framework of the WAME project, which is mainly devoted to the assessment and validation of the MOCABA data assimilation procedure and to the application to the analyses of the radiological ST during SAs in NPPs.

CRediT authorship contribution statement

A. Stakhanova: Conceptualization, Software, Writing – original draft, Visualization. **F. Gabrielli:** Conceptualization, Writing – review & editing, Supervision. **V.H. Sanchez-Espinoza:** Conceptualization, Writing – review & editing, Supervision, Project administration, Funding acquisition. **A. Hoefer:** Formal analysis, Writing – review & editing. **E. Pauli:** Formal analysis, Writing – review & editing.

Declaration of Competing Interest

The authors declare that they have no known competing financial interests or personal relationships that could have appeared to influence the work reported in this paper

Acknowledgements

The project was funded by the German Federal Ministry for Economic Affairs and Climate Action (BMWi), funding code FZK 1501582 (WAME project).

References

Kloos, M., Hofer, E., 1999. SUSA Version 3.2. User's Guide and Tutorial. GRS, Garching.

Chevalier-Jabet, K., Cousin, F., Cantrel, L., Séropian, C., 2014. Source term assessment with ASTEC and associated uncertainty analysis using SUNSET tool. Nucl. Eng. Des. 272, 207–218.

Blanchard, J.-B., Damblin, G., Martinez, J.-M., Arnaud, G., Gaudier, F., 2019. The Uranie platform: an open-source software for optimisation, meta-modelling and uncertainty analysis. EPJ Nuclear Sci. Technol. 5, 4. https://doi.org/10.1051/epjn/2018050.

Adams, B.M., et al. "2014, "Dakota, a Multilevel Parallel Object-Oriented Framework for Design Optimization, Parameter Estimation, Uncertainty Quantification, and Sensitivity Analysis: Version 6.0 User's Manual," Sandia National Laboratories, Albuquerque, NM, Report No." *SAND2014-4633*.

Hoefer, A., Buss, O., Hennebach, M., Schmid, M., Porsch, D., 2015. MOCABA: A general Monte Carlo-Bayes procedure for improved predictions of integral functions of nuclear data. Ann. Nucl. Energy 77, 514–521.

"MUSA Management and Uncertainties of Severe Accidents, European H2020 Project", (Accessed 2021, November 12), http://musa-h2020.eu/

Herranz, L.E. et al., 2020. First Steps of the EC-MUSA Project on Management and Uncertainty of Severe Accidents. Conference on Best estimate Modelling Plus Uncertainties in Safety Analyses BEPU-2020.

"Advancing the State-of-Practice in Uncertainty and Sensitivity Methodologies for Severe Accident Analysis in Water-Cooled Reactors", (Accessed 2021, November 12), https://www.iaea.org/projects/crp/i31033

Stuckert, J., Boldyrev, A.V., Miassoedov, A., 2005. *Experimental and computational results of the QUENCH-08 experiment (reference to QUENCH-07)*. No. FZKA–6970. Forschungszentrum Karlsruhe GmbH Technik und Umwelt (Germany). Inst. fuer Materialforschung.

Chatelard, P., Reinke, N., Arndt, S., Belon, S., Cantrel, L., Carenini, L., Chevalier-Jabet, K., Cousin, F., Eckel, J., Jacq, F., Marchetto, C., Mun, C., Piar, L., 2014. ASTEC V2 severe accident integral code main features, current V2.0 modelling status, perspectives. Nucl. Eng. Des. 272, 119–135.

McKay, M.D., Beckman, R.J., Conover, W.J., 1979. A comparison of three methods for selecting values of input variables in the analysis of output from a computer code. Technometrics 21 (2), 239–245.

Gómez-García-Toraño, I., Sánchez-Espinoza, V.-H., Stieglitz, R., Stuckert, J., Laborde, L., Belon, S., 2017. Validation of ASTECV2.1 based on the QUENCH-08 experiment. Nucl. Eng. Des. 314, 29–43.

Kobzar, V. et al., 1997. Uncertainty and Sensitivity Analysis of CORA-W2 Test Using ICARE2/SUNSET Tool, NSI RRC KI 2127. Russia, December, Moscow.

Gabrielli, F., Sanchez, V. "Uncertainty and Sensitivity Analysis by means of ASTEC/URANIE Platform of the QUENCH-08 Experiment", Proceedings of the 24th International QUENCH Workshop, pp. 354-375, Karlsruhe, Germany, November 2018.

Belon, S., et al. *Draft Manual for ASTEC V2. 1: ICARE Module. User manual. Rapport no PSN-RES*. SAG/2016-00421, 2017.

Coindreau, O. "ASTEC V2. 1: physical modelling of the ICARE module." *IRSN, Fontenay-aux-Roses, France, PSNRES/SAG/2016-00422* (2017).

de Luze, O., Haste, T., Barrachin, M., Repetto, G., 2013. Early phase fuel degradation in Phébus FP: Initiating phenomena of degradation in fuel bundle tests. Ann. Nucl. Energy 61, 23–35.

Wilks, S.S., 1941. Determination of sample sizes for setting tolerance limits. Ann. Math. Stat. 12 (1), 91–96.

Wald, A., 1943. An extension of Wilks' method for setting tolerance limits. Ann. Math. Statist. 14 (1), 45–55.

Tukey, J.W., 1947. Nonparametric estimation, II. Statistical equivalent blocks and tolerance regions - the continuous case. Ann. Math. Statist. 18 (4), 529–539.

SampleVis – Simple tool for sample visualization for sensitivity analysis (Accessed 2021, November 12), https://github.com/charlesrouge/SampleVis

Water Programming: A Collaborative Research Blog, Tips and tricks on programming, evolutionary algorithms, and doing research (Accessed 2021, November 12), https://waterprogramming.wordpress.com/2018/06/11/evaluating-and-visualizing-sampling-quality/

Sheikholeslami, R., Razavi, S., 2017. Progressive Latin Hypercube Sampling: An efficient approach for robust sampling-based analysis of environmental models. Environ. Modell. Software 93, 109–126.

pyDOE: The experimental design package for Python (Accessed 2021, November 12), https://pythonhosted.org/pyDOE/index.html

Gómez-García-Toraño, Ignacio. "Further development of Severe Accident Management strategies for a German PWR konvoi plant based on the European Severe Accident Code ASTEC." (2017).

Gabrielli, F, Sánchez-Espinoza, V.H., Stuckert, Gómez-García-Toraño, I., "VALIDATION OF THE ASTEC INTEGRAL CODE USING THE QUENCH-06 AND QUENCH-08 EXPERIMENTS", The 9th European Review Meeting on Severe Accident Research (ERMSAR2019), Clarion Congress Hotel, Prague, Czech Republic, March 18-20, 2019